Ne Emissions from a He Discharge Flow System: II. Products of the Reaction $He(2^1S) + Ne(1^1S)$

H. K. Haak, B. Wittig, and F. Stuhl
Ruhr-Universität, Physikalische Chemie I, Bochum, Germany

Z. Naturforsch. **35a**, 1342–1349 (1980); received November 20, 1980

A windowless He discharge was used to produce metastable singlet $He(2^1S)$ by the photolysis process $He(1^1S) + 58.4\ nm \rightarrow He(2^1P)$ and $He(2^1P) \rightarrow He(2^1S) + 2058\ nm$. Metastable $He(2^1S)$ were found to transfer their energy to Ne to populate the Ne 5s, 5s′, 4d, 4d′, 3d, and 3d′ states. In the present work the detailed relative population of these states and their rates of population are determined.

Introduction

The excitation transfer between metastable He and ground state Ne atoms has been previously recognized to be of fundamental importance to the generation of laser radiation in neon-helium systems [1]. Although electronic energy transfer reactions have been investigated for many years, a full characterization of the product states in the reactions of metastable $He(2^3S)$ and $He(2^1S)$ with Ne has not been achieved [2].

Previously, metastable He atoms have been produced by electron impact [3, 4] and by the afterglow discharge technique [5]. These methods yield either a mixture of triplet and singlet metastable He [3, 4] or triplet metastable He alone [5, 6], but the exclusive generation of $He(2^1S)$ appears to be difficult. In the present spectroscopic study we report a method for the generation of metastable singlet He and we infer a detailed product analysis for the reaction

$$He(2^1S) + Ne(1^1S) \rightarrow Ne^* + He(1^1S) \qquad (1)$$

from extensive emission spectra of Ne. In order to facilitate the understanding of the following sections a simplified energy level diagram of Ne [7] is displayed in Figure 1.

Experimental

The experimental method and procedure has been described in the preceding paper [8] and no details will be given here. Briefly, a windowless microwave discharge in He is used to irradiate mixtures of He and Ne in a flow system. The spectral emissions from this system were monitored by a monochromator using a photomultiplier and photon counting. The temperature of the gas in the flow tube was estimated from the rotational distribution of the N_2^+ (B→X) emission to be less than 390 K. This emission also indicates that air was always present in the flow system at a pressure of about 5 mTorr.

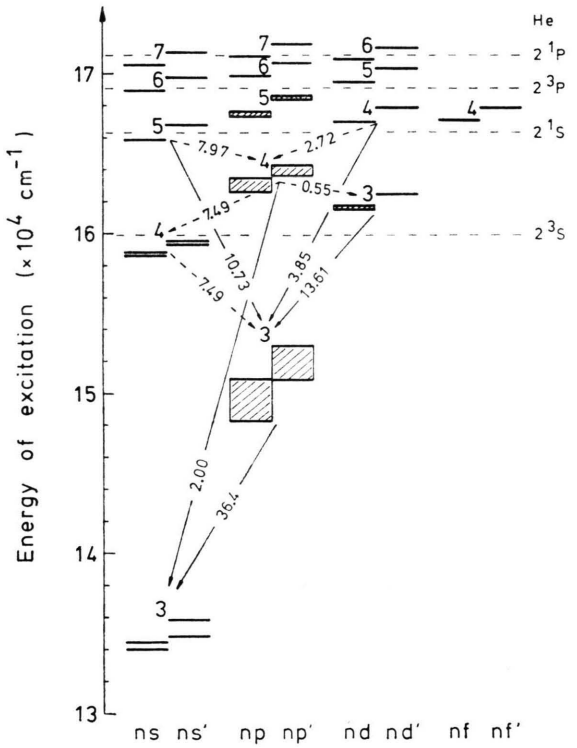

Fig. 1. Simplified energy level diagram of Ne. The observed and calculated relative intensities are indicated by full and dashed arrows (see text).

Reprint requests to Prof. Dr. F. Stuhl, Physikalische Chemie I, Ruhr-Universität Bochum, Postfach 102148, D-4630 Bochum 1, West Germany.

0340-4811 / 81 / 1200-1342 $ 01.00/0. — Please order a reprint rather than making your own copy.

Results

A large number of emission lines and several emission bands were observed in the flow tube with the discharge in position A (see Fig. 1 in [8]). Relatively weak emission bands from excited CO^+, CO_2^+ and N_2^+ ions and several lines from excited O and H atoms are still present when Ne is absent and are therefore considered to be caused by impurities in the flow system. Although the discharge region could not be viewed directly from the monochromator, several emission lines from He states of up to 195269 cm^{-1} excitation energy were observed. In the absence of Ne, the intensities of these He lines slightly decreased by 6 to 9% for the addition of 0.1 Torr He through inlet (c).

Upon addition of small amounts of Ne to the flow system through inlet (c), about 270 additional emission lines were observed in the wavelength range from 270 to 890 nm. All these observed emissions were identified by their corresponding Ne transitions [9]. Some experiments were performed with the discharge in position B and using inlet (b) for He (see Fig. 1 in [8]). With this position the intensities of the Ne emissions decrease by more than a factor of 40. In these experiments, light from the discharge could not irradiate the flow system directly. In another experiment, the emission intensities were found to be independent of the flow direction of He. Hence the presence of reactive species in the effluence of the He discharge cannot be a major cause for the Ne emissions observed.

As an example for the dependence of the Ne intensities on the pressure of Ne, Fig. 2 shows the pressure dependence of the Ne emission at 632.82 nm for the transition $(5s'(1/2)1 \rightarrow 3p'(3/2)2)$ [10]. All the other Ne emissions exhibit the same dependence. In these runs which were performed at a constant pressure of 0.9 Torr He the intensities of the Ne emissions increase rapidly upon the addition of small amounts of Ne until a nearly constant intensity is reached at about 0.07 Torr Ne. Also included in Fig. 2 are the photomultiplier signals for the four following selected He lines: 728.13 nm, $He(3^1S \rightarrow 2^1P)$; 587.56 nm, $He(3^3D \rightarrow 2^3P)$; 501.57 nm, $He(3^1P \rightarrow 2^1S)$; and 388.86 nm, $He(3^3P \rightarrow 2^3S)$. The corresponding He transitions connect upper excited states with the four lowest excited states of He, the 2^1S and 2^3S states of which

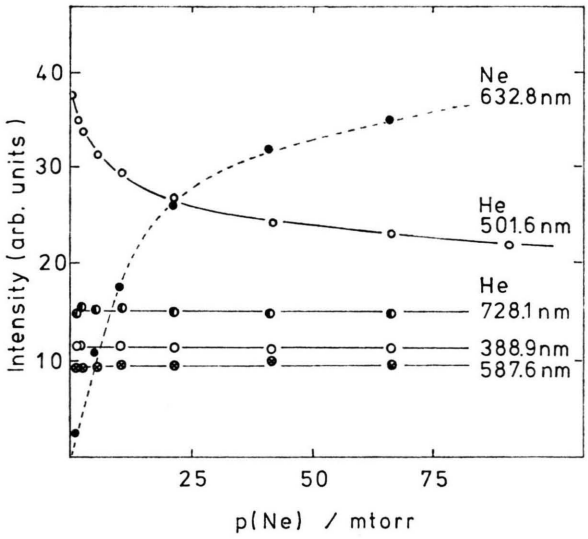

Fig. 2. The intensity of some emission lines as a function of pressure of Ne.

are metastable. Upon the addition of Ne, in Fig. 2, the intensity of the 501.57 nm He line decreases while the intensities of the other He lines remain constant.

Strong emission intensities ($\geqq 10\%$ of the strongest Ne line at 640.23 nm) are found to originate from the 4d, 5s', 3d', 3d, 3p', and 3p levels; weaker lines (intensities between 1% and 10% of the strongest line) are emitted from the 6d, 5d, 4d', 5s, 4p', and 4p levels; and very weak lines (intensities between 0.01% and 1% of the strongest line) are emitted from the 8s', 8s, 7d, 7p, 7s, 7s', 6d', 6p', 6p, 6s', 6s, 5d', 5p', and 5p levels.

Figure 3 summarizes the relative emission intensities observed in the wavelength range from 200 nm to 890 nm. In this figure, the sums of the observed intensities from all sublevels of a given quantum number *nl* oder *nl'* are displayed on a logarithmic scale as a function of excitation energy. Also included in this figure are the positions of the energy levels of the He states (2^1P), (2^1S), (2^3P), and (2^3S). It should be noted that this data in Fig. 3 does not represent all the emissions occuring in the investigated reaction system because of the limited wavelength range studied. For example, all the emission lines of the transitions (4s, 4s' → 3p, 3p') and some of the lines of the transitions (3d, 3d' → 3p, 3p') lie in the IR region outside the observed wavelength range. Figure 3 shows that the majority of the emissions is generated by transitions from the 3p,

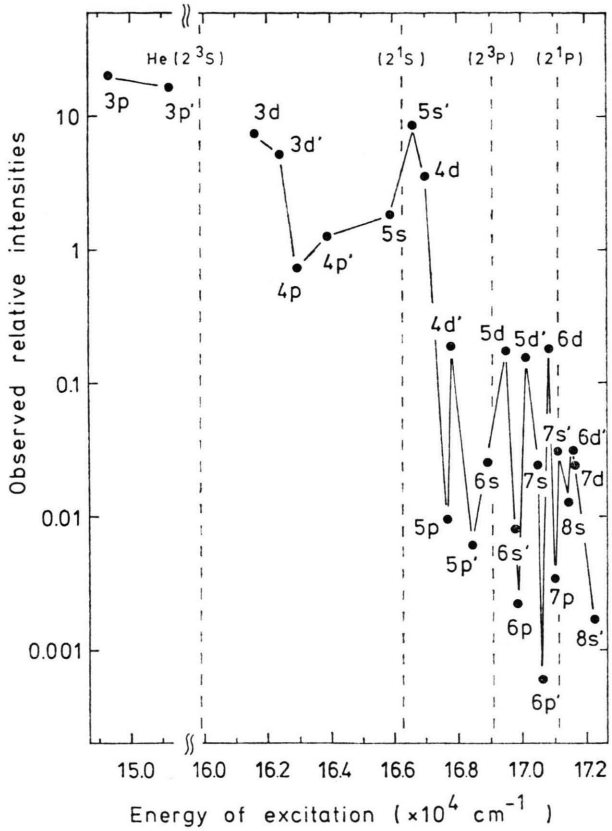

Fig. 3. A semilogarithmic plot of the observed intensities as a function of excitation energy.

3p', from the 3d, 3d', and from the 5s, 5s' and 4d levels. A plausible mechanism for the population of these energy levels will be discussed later. It should be noted that above an excitation energy of 167051 cm^{-1} (4d levels) only weak emissions are generated up to an Ne excitation energy of 172264 cm^{-1} (8s' levels).

Discussion

The energy transfer from metastable He atoms to Ne is known to be responsible for the generation of laser emissions in the He-Ne laser system and in a number of studies the corresponding energy transfer reactions have been investigated [2, 11—15].

The experimental system applied to produce Ne emissions in the present work is similar to the windowless He discharge system previously used by Back and Walker [16, 17] to study the photoionization of simple molecules by measuring ion currents. The major modification in the present study is the omission of the fast-flow separation system [16]. Those authors have previously suggested that both metastable He(2^1S) and He(2^3S) are produced by collisional conversion of the resonantly trapped He(2^1P) state. These metastable atoms have been proposed to interact with added gases such as Ne and CH_4 [16, 17].

The present experiments with different discharge positions and He flow directions strongly indicate that at least 98.5% of the observed Ne emission intensity is due to direct illumination of the flow tube by light from the He discharge. The most dominant emission from a discharge in He is the 58.4 nm resonance line [18]. Since Ne is transparent for this radiation the observed excitation should be due to collisions of the second kind. It is known that He resonance radiation is efficiently trapped leading to a relatively long lifetime of the He(2^1P) state [11, 16]. At the He pressures used the resonantly excited He(2^1P) atoms most likely decay to the metastable He(2^1S) state mainly by radiation after a lifetime of 5.3×10^{-7} s [19]. We therefore propose the following excitation mechanism to occur in the present flow system:

$$\mathrm{He}(1^1S) + 58.4\ \mathrm{nm} \leftrightarrow \mathrm{He}(2^1P), \quad (2)$$

$$\mathrm{He}(2^1P) \rightarrow \mathrm{He}(2^1S) + 2058\ \mathrm{nm}, \quad (3)$$

$$\mathrm{He}(2^1S) + \mathrm{Ne}(1^1S) \rightarrow \mathrm{Ne}^* + \mathrm{He}(1^1S). \quad (1)$$

Support for the presence of metastable He(2^1S) atoms is obtained by the data displayed in Figure 2. Namely, the marked decrease of the scattered light intensity of the He($3^1P \rightarrow 2^1S$) emission at 501.57 nm in Fig. 2 can be explained to be due to quenching of resonance fluorescence by added Ne. It is well known that Ne rapidly reacts ($k = 6.46 \times 10^{-11}$ $cm^3\ s^{-1}$ at room temperature [20]) with He(2^1S) and thus very effectively reduces the concentration of metastable atoms. Consequently, at large Ne concentrations, resonance fluorescence of He(2^1S) cannot be generated and only light scattered at the walls of the flow system is detected. Furthermore, from the nearly constant He intensities at 728.13, 587.56, and 388.86 nm in Fig. 2 it can be inferred that no resonance fluorescence emission of the He(2^1P), (2^3P), and (2^3S) states is observed. From the intensities and the corresponding transi-

tion probabilities [21] for these four scattered emission lines, we estimate the sensitivity for the fluorescence detection of He(2^1P), (2^3S), and (2^3P) to be not lower than that of He(2^1S). On this basis the concentrations of excited He produced in the (2^1P), (2^3S), and (2^3P) states are at least one order of magnitude lower than the concentration of metastable singlet He(2^1S). Moreover, the shape of the curves of both the 501.6 nm He and the Ne intensity in Fig. 2 can be quantitatively understood by the competition of Ne with residual air (at about 5 mTorr) for the reaction with He(2^1S).

The presence of metastable singlet He atoms as a major light producing species can be also inferred from the observed intensity distribution of the Ne emissions displayed in Figure 3. This figure clearly demonstrates that, to a major extend, cascading of radiation originates in the Ne(4d, 5s′, 5s) states. These states are almost in resonance with the He(2^1S) state. Figure 3 furthermore shows that Ne states with higher energies than that of the 4d states are populated. The emission intensities from these states, however, are one to four orders of magnitude lower than the intensity from the 4d states. It is interesting to note that of all these highly excited Ne states the d and d′ states generally emit much stronger than the other states and that the p and p′ states generally emit very weakly. Moreover, the emission intensity decreases remarkably above the energy of excitation of He(2^1P). It therefore appears to be likely that these states are excited by resonantly trapped He(2^1P) atoms. Whether He(2^1P) is the only source of excitation for these highly excited Ne states cannot be decided here and the population of these weakly populated Ne states will not be further discussed.

The relative population of the individual 4d′, 4d, 5s′, 5s, 4p′, 4p, 3d′, and 3d states was calculated using the observed relative intensities and the corresponding previously calculated transition probabilities [22—26]. Usually, for the calculation of the population of each neon state, one of the strongest line of its emission array was used. However, care was taken that no emission line above 850 nm was used because of the uncertainty in the optical sensitivity at these wavelengths. Furthermore, lines which coincide with other lines were avoided. Table 1 displays the relative population for the individual 5s′, 5s, 4d′, and 4d states. It is evident from this table that the highest population

Table 1. Relative population of excited Ne in the 5s, 5s′ and 4d, 4d′ states.

State	Energy (cm^{-1})	Relative population this work	Ref. [28]	Ref. [27]	Ref. [14]
5s′ (1/2) 1[a]	166658.48	1.23	1.23	1.23	1.23
5s′ (1/2) 0	166608.31	0.0063	0.068	0.0003	< 0.025
5s (3/2) 1	165914.76	0.137	0.12	0.001	0.33
5s (3/2) 2	165830.14	0.125	0.12	0.002	0.24
4d′ (3/2) 1[b]	167809.72	0.0031			
4d′ (3/2) 2	167798.91	0.0036			
4d′ (5/2) 3	167797.87	0.0061			
4d′ (5/2) 2	167796.94	0.0047			
4d (5/2) 3	167050.64	0.0568			
4d (5/2) 2	167049.58	0.0397			
4d (3/2) 1	167028.96	0.0304			
4d (3/2) 2	167013.54	0.0526			
4d (7/2) 3	167003.10	0.0821			
4d (7/2) 4	167002.01	0.103			
4d (1/2) 1	166977.32	0.0393			
4d (1/2) 0	166969.64	0.0106			

[a] For the 5s′ and 5s states the transition probabilities were taken from Ref. [24].
[b] For the 4d′ and 4d states the transition probabilities were taken from Ref. [25].

is observed for the 5s′ (1/2)1 state. On the other hand the 5s′ (1/2)0 state has a population which is as small as those of the 4d′ states. The average population of the 5s states is found to be about 2.5 times larger than the average population in the 4d states. It is interesting to compare the present population distribution with those given in the literature for Reaction (1). To our knowledge only values for the population distribution of the 5s′, 5s states have been reported [14, 27, 28]. These values are shown in Table 1. There is general agreement that the 5s′(1/2)1 state is dominantly and that the 5s′(1/2)0 state is barely populated [14, 27, 28]. Furthermore each of the 5s states contains about 10% of the population of the 5s′(1/2)1 state [28]. This distribution has been extensively discussed previously [11, 14, 15], and here we will rather emphasize the distribution observed in the 4d′, 4d, 3d, and 3d′ states.

Previously, it has been assumed that the 4d states are populated by energy transfer from the He($2^3P_{0,1,2}$) states [11, 29]. Recently, using atomic beam technique and time of flight measurements, the production of Ne(4d) states has been observed in an investigation of the energy dependence of Reaction (1) [15]. Although, because of lack of energy resolution, no detailed population distribu-

tion has been obtained in those experiments the present results confirm those of the beam study. Namely, under the conditions of the present study, all the 4d states together contain about one third of the population of the 5s′(1/2)1 state. The distribution in the 4d states is very different from that in the 5s′ states. While the population in the 5s′ states varies by a factor of 200 the population in the 4d states differs by no more than one order of magnitude. It should be noted that the 4d state with the largest population is the 4d(7/2)4 state which lies 730.3 cm^{-1} above the He(2^1S) state and 32.4 cm^{-1} above the lowest 4d state.

Table 2 summarizes the population distribution observed for the 4p′, 4p, 3d′, and 3d states. As will be calculated later the 4p′ and 4p states are dominantly populated by transitions from the 5s′, 5s, 4d′, and 4d states. The 3d and 3d′ states, however, are most likely generated directly in Reaction (1) as will be discussed later.

The high population of the nearly resonant 5s′, 5s, and 4d states implies that these states are products of different channels of Reaction (1). In order to estimate the relative rates of these reaction channels we have determined the relative fluxes of the radiation cascade originating in these states. Under the assumption of negligible quenching of the excited neon by ground state helium and under the assumption of complete trapping of the radiation from those Ne states which are radiatively connected with the ground state, the radiative flux can be taken as a direct measure for the rate of population. These assumptions seem to be valid since He is generally found to be an inefficient quencher. Furthermore, the radiative lifetime of the observed Ne states are close to 10^{-7} s. Thus, it seems to be unlikely that quenching by He competes efficiently with radiative deexcitation in the present system. Radiation trapping in Ne has been commonly accepted for He-Ne laser systems [11, 28] and hence transitions to the Ne ground state are not likely to reduce the cascading radiation significantly.

Table 3 summarizes the relative radiative fluxes from the Ne 5s′, 5s, 4d, and 4d′ levels. The sum of the relative intensities (relative number of photons per area and time) of all emission lines from a

Table 2. Relative population of excited Ne in the 3d, 3d′ and 4p, 4p′ states.

State	Energy (cm^{-1})	Relative population
3d′ (3/2) 1[a]	162437.64	0.022
3d′ (3/2) 2	162421.94	0.024
3d′ (5/2) 3	162412.14	0.044
3d′ (5/2) 2	162410.62	0.025
3d (5/2) 3	161703.41	0.035
3d (5/2) 2	161701.62	0.025
3d (3/2) 1	161638.58	0.012
3d (3/2) 2	161609.22	0.017
3d (7/2) 3	161594.08	0.034
3d (7/2) 4	161592.31	0.039
3d (1/2) 1	161526.13	0.009
3d (1/2) 0	161511.59	0.003
4p′ (1/2) 0[b]	164287.86	0.251
4p′ (3/2) 2	163710.58	~ 0.3
4p′ (1/2) 1	163709.70	0.125
4p′ (3/2) 1	163659.25	0.097
4p (1/2) 0	163403.28	0.041
4p (3/2) 2	163040.33	0.104
4p (3/2) 1	163014.60	0.048
4p (5/2) 2	162901.09	0.061
4p (5/2) 3	162832.68	0.093
4p (1/2) 1	162519.85	0.008

[a] For the 3d′ and 3d states the transition probabilities were taken from Ref. [26].

[b] For the 4p and 4p′ states the transition probabilities were taken from Ref. [23].

Table 3. Relative radiative fluxes from the 5s, 5s′ and 4d, 4d′ states of Ne.

From state	Flux to states: 3p, 3p′[a]	Flux to states: 4p, 4p′[b]	Sum of fluxes	Relative cross Sections, Ref. [14]
5s′ (1/2) 1	8.78	6.53	15.31	15.31 ± 0.15
5s′ (1/2) 0	0.041	0.035	0.076	< 0.09 ± 0.045
5s (3/2) 1	0.978	0.727	1.705	4.9 ± 0.15
5s (3/2) 2	0.930	0.678	1.602	1.1 ± 0.05
4d′ (3/2) 1	0.024	0.019	0.043	
4d′ (3/2) 2	0.034	0.024	0.058	
4d′ (5/2) 3	0.079	0.038	0.117	
4d′ (5/2) 2	0.044	0.030	0.074	
4d (5/2) 3	0.498	0.348	0.846	
4d (5/2) 2	0.351	0.243	0.594	
4d (3/2) 1	0.203	0.145	0.348	
4d (3/2) 2	0.482	0.353	0.835	
4d (7/2) 3	0.733	0.510	1.243	
4d (7/2) 4	0.938	0.678	1.616	
4d (1/2) 1	0.354	0.258	0.612	
4d (1/2) 0	0.106	0.077	0.183	

[a] All the corresponding transitions to the 3p and 3p′ states were observed.

[b] All the corresponding radiative fluxes were calculated using the relative population of Table 1 and the transition probabilities of Ref. [24] for the 5s′ and 5s states and of Ref. [22] for the 4d′ and 4d states.

given Ne state is taken as a measure for the flux from this state. It should be noted in Table 3 that all the emissions of the transitions to the 3p and 3p′ states were observed while the corresponding emissions to the 4p and 4p′ states lie in the IR and, hence, their intensities had to be calculated. This was done using the relative population distribution of Table 1 and known transition probabilities [22, 24]. Included in Table 3 are recent data [14] of relative cross sections for the formation of Ne in the 5s, 5s′ states. A comparison of this data with the present values of the corresponding fluxes reveals significant differences which might be caused by the different reaction energy (broad energy spread around 60 meV) used in this beam experiment [14]. Table 3 clearly shows that the most dominant channel of Reaction (1) leads to the population of 5s′(1/2)1. Furthermore, there are two Ne 4d levels which are almost as efficiently formed as the two 5s levels, namely 4d(7/2)3 and 4d(7/2)4. On the average a 4d and a 4d′ level becomes 20 times and 200 times less efficiently populated than the 5s′(1/2)1 level. This decreased average population rate for these upper Ne states roughly corresponds to the increased endothermicity of the formation of the 4d and 4d′ states in Reaction (1). It should be noted, however, that the individual 4d and 4d′ energy levels are not at all populated according to their energetic positions and hence a particular selection mechanism must exist.

The observed intensities shown in Fig. 3 indicate that also the 3d′ and 3d states are populated very efficiently. The radiative fluxes from the individual 3d′ and 3d states were therefore determined using the observed emission intensities. Since a few lines of the (3d→3p, 3p′) arrays emit in the near infrared their intensities were calculated using known transition probabilities [26]. This correction amounted to a small overall increase of 9% in the flux from the 3d levels. The relative radiative fluxes from the 3d′ and 3d levels are listed in Table 4.

The fluxes of radiation created in the 4d′, 4d, 5s′, 5s, 3d′, and 3d states cascade down via the 4p′, 4p, 3d′, 3d, 4s′, 4s, 3p′, and 3p states to the 3s and 3s′ states. The relative intensities (fluxes) of this radiation cascade are summarized in Table 5. Several values of this table were calculated using the population distribution given in Table 1 and 2

Table 4. Relative radiative fluxes from the 3d, 3d′ states to the 3p, 3p′ states.

State	Flux[a]
3d′(3/2)1	0.952
3d′(3/2)2	1.268
3d′(5/2)3	1.894
3d′(5/2)2	1.274
3d(5/2)3	1.660
3d(5/2)2	1.045
3d(3/2)1	0.461
3d(3/2)2	1.012
3d(7/2)3	1.481
3d(7/2)4	1.940
3d(1/2)1	0.457
3d(1/2)0	0.170

[a] Almost all the corresponding emissions were observed. A correction is applied for some IR emission lines using the data of Table 2 and transition probabilities of Ref. [26].

and known transition probabilities [22, 23, 26]. For the (4s, 4s′→3p, 3p′) transitions it is assumed that the corresponding radiative flux is equal to that of the transitions (4p, 4p′→4s, 4s′). The relative flux for the transitions (4p, 4p′→3d, 3d′) was estimated to be only 0.55, since the corresponding transition probabilities are small [22]. The fluxes of Table 5 are also indicated in Fig. 1 by full and dashed arrows for the observed and calculated intensities, respectively.

The data of Table 5 confirm that the 3d′ and 3d states are a major source of radiation in this system. These Ne states are far from being in resonance with any He state and their population from highly excited states has to be considered. But the Ne $np, np'(n>4)$ states are only weakly populated as

Table 5. Radiation budget expressed by the state to state radiative fluxes.

From states	To states	Relative radiative flux
4d, 4d′ →	4p, 4p′	2,72[a]
4d, 4d′ →	3p, 3p′	3.85[a]
5s, 5s′ →	4p, 4p′	7,97[a]
5s, 5s′ →	3p, 3p′	10.73[a]
4p, 4p′ →	3d, 3d′	0.55[c]
4p, 4p′ →	4s, 4s′	7.49[c]
4p, 4p′ →	3s, 3s′	2.00[d]
3d, 3d′ →	3p, 3p′	13.61[b]
4s, 4s′ →	3p, 3p′	7.49[e]
3p, 3p′ →	3s, 3s′	36.4[d]

[a] From the data of Table 3.
[b] From the data of Table 4.
[c] Calculated using the relative population given in Table 2 and the known transition probabilities for radiation to the 4s, 4s′ states [23] and to the 3d, 3d′ states [22].
[d] All the corresponding intensities were observed.
[e] The radiative flux for (4s, 4s′→3p, 3p′) is taken to be equal to that for the transitions (4p, 4p′→4s, 4s′).

Fig. 3 indicates and these states can barely contribute to the large rate of population of the 3d, 3d′ states. The 3d, 3d′ states could be also populated by transitions from the nf, nf' manifold. The presence of these excited atoms cannot be detected with the present optical arrangement since they emit too far in the IR region. The lowest of these states, the 4f states lie 796 ± 12 cm^{-1} above the energy of He(2^1S). This energy range is slightly above the range of endothermicity of the Ne(4d) states (736.5 ± 40.5 cm^{-1}) and hence the generation of 4f states is not expected to be much more efficient than that of the 4d states. Therefore, we conclude that most of the 3d, 3d′ emissions observed must originate in these states by Reaction (1) directly. Thus, the present emission spectroscopy study is in support of crossed beam time-of-flight measurements which show that highly exoergic Ne* corresponding to 3d atoms are formed [12].

Since the contributions to the population of the 3d and 3d′ states from upper excited Ne states appear to be small, the fluxes given in Table 4 are likely to represent the relative rates of population of the 3d and 3d′ states in Reaction (1). It is therefore interesting to compare the data of Table 4 with the corresponding data for the 4d′ and the 4d states (Table 3). This comparison reveals that the rates of population of the 4d states are smaller than those for the 3d states and that the rates of population of the 4d′ states are very much smaller than those of the 3d′ states. This is probably due to the energetic positions of these states. On the other hand, the distribution of the rate of population in the 3d′ states resembles very much that of the 4d′ states. The same fact is noticed when comparing the rate of population of the 3d states with that of the 4d states.

The budget of the radiation flux (Table 5) can be checked reasonably well for the 4p, 4p′ states and for the 3p, 3p′ states which can be considered to be bottlenecks. The data of Table 5 shows that the fluxes to and from the 4p and 4p′ states agree within 6.4%. The fluxes to and from the 3p and 3p′ states agree within 2% which is well within the error limit of the present work. This radiation budget indicates that within the error limits, no additional excited Ne atoms in the 4s and 4s′ states are created. Particularly it is well known that metastable triplet He(2^3S) efficiently excite Ne to the 4s, 4s′ states [11]. Hence, no indication of the presence of He(2^3S) is given from the present spectroscopic data.

The concentration of metastable triplet He(2^3S) is thought to be low in the present system ([He(2^1S)] $> 10 \times$ [He(2^3S)]), because of the following reasons: Metastable He(2^3S) generated in the discharge region can hardly reach the observed volume since it takes about 50 ms for the flow to reach the observed reaction volume. Furthermore, the gases used contained air at a partial pressure of about 5 mTorr (caused by permeation through the plastic tubings and by leaks). The lifetime of He(2^3S) in the presence of this amount of air is about 60 μs which is a factor of 10^3 smaller than the time to reach the observed volume. Using the split flow arrangement (see Fig. 1 in [8], dashed arrows) the time to reach the observed volume is further increased without effecting the emission intensities of Ne. Similar arguments are valid for the transport of singlet metastable He(2^1S) from the discharge. It is therefore most likely that the reactive species are formed downstream photolytically as demonstrated by the results using different positions of the resonator. This process of formation is indicated above by reactions (1)—(3) thus favoring excited singlet species.

In the presence of Ne at 0.1 Torr the lifetimes of He(2^3S) and of He(2^1S) are about 80 μs and about 5 μs, respectively. For the slow flow velocity of the present system these lifetimes result in reactions on the spot and about half of the He(2^3S) is expected to react with Ne. However, no indication of this reaction is observed.

Finally, no resonance fluorescence of He(2^3S) is observed (Figure 2). Addition of Ne and also of N_2 and CO decreases the intensity of the 501.6 nm He line and also of other emissions of transitions ending in the metastable He(2^1S) level. However, no decrease of intensity of the 388.9 nm He line and of other emissions of transitions ending in the metastable He(2^3S) level is observed.

Acknowledgement

We gratefully acknowledge financial support of the Deutsche Forschungsgemeinschaft. We also thank Prof. Dr. H. Haberland for providing us with the Diplomarbeit of W. Konz and with the Dissertation of P. Oesterlin and for bringing to our attention the work of J. Krenos.

[1] R. J. Pressley, Ed., "Handbook of Lasers with Selected Data on Optical Technology", Chemical Rubber Co., Cleveland 1971.
[2] D. L. King and D. W. Setser, Ann. Rev. Phys. Chem. **27**, 407 (1976).
[3] V. Čermák, J. Chem. Phys. **44**, 3781 (1966).
[4] E. E. Muschlitz, Jr., Adv. Chem. Phys. **10**, 171 (1966).
[5] W. W. Robertson, J. Chem. Phys. **44**, 2456 (1966).
[6] A. L. Schmeltekopf, E. E. Ferguson, and F. C. Fehsenfeld, J. Chem. Phys. **48**, 2966 (1968).
[7] S. Bashkin, J. O. Stoner, Jr. "Atomic Energy Levels and Grotrian Diagrams", Vol. 1, North Holland Pub. Co. Amsterdam 1975.
[8] H. K. Haak, C. Zetzsch, and F. Stuhl, preceding paper.
[9] A complete list of these lines including wavelengths, states, energies of upper states, and relative intensities can be obtained from the authors.
[10] Throughout this paper the Racah notation will be used.
[11] C. S. Willett "Introduction to Gas Lasers: Population Inversion Mechanisms", Pergamon Press, Oxford 1974.
[12] D. W. Martin, T. Fukuyama, R. W. Gregor, R. M. Jordan, and P. F. Siska, J. Chem. Phys. **65**, 3720 (1976).
[13] H. Haberland, P. Oesterlin, and K. Schmidt, Ber. Bunsenges. Phys. Chem. **81**, 184 (1977).
[14] J. Krenos, Abstracts of Papers, Seventh Int. Symp. on Molecular Beams, Riva del Garda, Italy, 1979.
[15] H. Haberland, private communication. — W. Konz, Diplomarbeit, Freiburg 1978. — P. Oesterlin, Dissertation, Freiburg 1979.
[16] R. A. Back and D. C. Walker, J. Chem. Phys. **37**, 2348 (1962).
[17] D. C. Walker and R. A. Back, J. Chem. Phys. **38**, 1526 (1963).
[18] J. A. R. Samson, Techniques of Vacuum Ultraviolet Spectroscopy, John Wiley, New York 1967.
[19] M. G. Payne, C. E. Klots, and G. S. Hurst, J. Chem. Phys. **63**, 1422 (1975).
[20] A. L. Schmeltekopf and F. C. Fehsenfeld, J. Chem. Phys. **53**, 3173 (1970).
[21] W. L. Wiese, M. W. Smith, and B. M. Glennon, Atomic Transition Probabilities, Nat. Stand. Ref. Data Ser., NBS **4**, Vol. 1 (1966).
[22] P. W. Murphy, J. Opt. Soc. Amer. **58**, 1200 (1968).
[23] A. V. Loginov and P. F. Gruzdev, Opt. Spectrosc. **39**, 464 (1975).
[24] R. A. Lilly, J. Opt. Soc. Amer. **65**, 389 (1975).
[25] R. A. Lilly, J. Opt. Soc. Amer. **66**, 971 (1976).
[26] R. A. Lilly, J. Opt. Soc. Amer. **66**, 245 (1976).
[27] J. T. Massey, A. G. Schulz, B. F. Hochheimer, and S. M. Cannon, J. Appl. Phys. **36**, 658 (1965).
[28] R. T. Young, Jr., C. S. Willett, and R. T. Maupin, J. Appl. Phys. **41**, 2936 (1970).
[29] L. Colombo, B. Marković, Ž. Pavlović, and A. Peršin, J. Opt. Soc. Amer. **56**, 890 (1966).